Flash Pyrolysis of Ethyl, *n*-Propyl, and Isopropyl Iodides as Monitored by Supersonic Expansion Vacuum Ultraviolet Photoionization Time-of-Flight Mass Spectrometry

Kevin H. Weber, Jessy M. Lemieux, and Jingsong Zhang*

Department of Chemistry, University of California, Riverside, California 92521

Received: September 13, 2008; Revised Manuscript Received: November 17, 2008

The thermal decomposition of ethyl and propyl iodides, along with select isotopomers, up to 1300 K was performed by flash pyrolysis with a 20−100 μs time scale. The pyrolysis was followed by supersonic expansion to isolate the reactive intermediates and initial products, and detection was accomplished by vacuum ultraviolet single photon ionization time-of-flight mass spectrometry (VUV-SPI-TOFMS). The products monitored, such as CH_3, CH_3I, C_2H_5, C_2H_4, HI, I, C_3H_7, C_3H_6, and I_2, provide for the simultaneous and direct observation of molecular elimination and bond fission pathways in ethyl and propyl iodides. In the pyrolysis of ethyl iodide, both C−I bond fission and HI molecular elimination pathways are competitive at the elevated temperatures, with C−I bond fission being preferred; at temperatures ≥1000 K, the ethyl radical products further dissociate to ethene + H atoms. In the pyrolysis of isopropyl iodide, both HI molecular elimination and C−I bond fission are observed and the molecular elimination channel is more important at all the elevated temperatures; the isopropyl radicals produced in the C−I fission channel undergo further decomposition to propene + H at temperatures ≥850 K. In contrast, bond fission is found to dominate the *n*-propyl iodide pyrolysis; at temperatures ≥950 K the *n*-propyl radicals produced decompose into methyl radical + ethene and propene + H atom. Isotopomer experiments characterize the extent of surface reactions and verify that the HI molecular eliminations in ethyl and propyl iodides proceed by a C1, C2 elimination mechanism (the 1,2 intramolecular elimination).

Introduction

The dehydrohalogenation of alkyl halides have been extensively studied[1] and are initiated by either homolytic fission of the carbon-halogen bond or 1,2 intramolecular elimination (ϵ_i). Although alkyl fluorides are resistant to dehydrohalogenation,[1−3] alkyl chlorides and bromides form alkene and hydrogen halide cleanly over intermediate temperatures, predominately by 1,2-ϵ_i, a process that continues to attract theoretical interest.[4−6] Alkyl iodide pyrolysis has proven more complicated than for other alkyl halides, long being known to produce a melange of alkene, alkane, and molecular iodine.[7] The saturated compound and iodine are formed by the fast reaction of hydrogen iodide and radicals with alkyl halide. The weaker C−I bond results in greater competition between bond fission and ϵ_i initiation events.

The first quantitative kinetic measurements for the thermal decomposition of alkyl iodides were made by Ogg and Jones for isopropyl[8] and *n*-propyl[9] iodides. Isopropyl iodide was found to obey first order kinetics, and although both radical and molecular mechanisms were postulated, at that time the relative contributions of bond fission and molecular elimination were not accessible. However, in a subsequent study of bond dissociation energies for organic iodides, Butler and Polanyi[10] interpreted their results by considering both bond fission and molecular elimination pathways as partially rate determining. In contrast to isopropyl iodide, *n*-propyl iodide decomposed with a rate law order of 1.5 (rate = $k[CH_3CH_2CH_2I][I]^{0.5}$) indicating the importance of radical chemistry. Later, Benson and co-workers[11−23] studied extensively the pyrolysis of alkyl iodides and believed the rate-determining step to be formation of hydrogen iodide. The rate law for *n*-propyl iodide being of order 1.5 was then understood as HI formation resulting from secondary hydrogen abstraction by an iodine atom following bond fission. They confirmed that isopropyl iodide has a first order rate law[19] and undergoes elimination faster than iodine atom attack. The change in mechanism is explained in terms of (1) a stronger primary C−H bond, rendering H abstraction less facile and (2) attenuation of the activation energy for the molecular elimination. Although a true carbocation does not form in the gas phase, a strong correlation between heterolytic bond energies and activation energies for 1,2-ϵ_i has been demonstrated.[24] The semi-ion transition state[22,23] is highly polar and carbocation character is stabilized by polarizable alkyl groups, in a situation akin to the regioselectivity observed in (the reverse reaction) Markovnikov addition to alkenes. This is illustrated by the α-CH_3 effect,[22] where it was documented that each additional α-CH_3 results in an ∼25 ± 4 kJ/mol reduction of activation energy for dehydrohalogenation. Ethyl iodide also decomposes according to a first order rate law.[20] Benson et al. believed that, although "surprising" due to being a primary alkyl halide, the pyrolysis of ethyl iodide was completely consistent with the rate determining step being molecular elimination, yet they did not exclude the possibility of up to 20% radical dispropriation. It was argued at this time that the pyrolysis of alkyl iodides proceeded primarily by either one of two mechanisms, a radical mechanism, associated with primary iodides (except ethyl iodide), or 1,2-ϵ_i, associated with secondary and tertiary iodides.

Yang and Conway[25] attempted first to separate measurements of bond fission and molecular elimination rates for alkyl halides with ethyl iodide using a toluene flow technique over the temperature range of 660 − 794 K. They argued that ethyl

* Corresponding author. Fax: (951) 827-4713. E-mail: jingsong.zhang@ucr.edu. Also at Air Pollution Research Center, University of California, Riverside, CA 92521.

10.1021/jp808155a CCC: $40.75
Published on Web 12/17/2008

radicals created immediately reacted with toluene in the flow system and by monitoring the production of ethene and ethane, both rates were elucidated. Their work indicated approximately 70% of the reaction proceeded via bond fission over this temperature range. The work was considered inconclusive,[26] and it was suggested that the bond fission pathway may contribute only ~2−20%. In comparison, more recently both Herzler and Frank[27] and Mertens et. al[28] considered the molecular elimination pathway to be negligible. The pyrolysis of ethyl iodide was recently studied by Kumaran et. al[29] with a shock tube coupled to atomic resonance absorption spectrometry (ARAS), directly observing H atoms over the temperature range of 1080−2020 K and iodine atoms over the temperature range of 946−2046 K. Using the directly measured bond fission rates analyzed with RRKM statistical theory and available experimental data, they demonstrated that the reaction proceeds predominantly via the radical mechanism (C−I fission) with a branching fraction of 0.87 ± 0.11 in relation to molecular elimination. The resulting ethyl radical is unstable (in fact, this reaction has been used as a H atom source) and rapidly decomposes to ethene and H atom. The most recent study on the pyrolysis of ethyl iodide was by Miyoshi et. al,[30] also using a shock tube coupled to ARAS detection of I atoms in the temperature range of 950−1400 K with analysis by RRKM statistical theory. They reported a C−I fission branching fraction of 0.92 ± 0.06, in good agreement with that by Kumaran et al.[29]

King,[21] under Benson, reported the very low pressure pyrolysis (VLPP) for *n*-propyl and isopropyl iodides in 1971. In the VLPP experimental regime the *n*-propyl radicals rapidly decompose to form methyl radical and ethene. By monitoring the rates of propene and ethene formation kinetic parameters for both 1,2-ϵ_i and C−I bond fission were elucidated for *n*-propyl iodide, while the decomposition of isopropyl iodide was considered to proceed completely by 1,2-ϵ_i. The decomposition of C3 and C4 alkyl iodides have been recently examined by Miyoshi et. al[30] using a shock tube coupled to ARAS detection of I atoms over the temperature range of 950−1400 K. They determined the C−I bond fission branching ratios of 0.6−0.9 for primary iodides, 0.2−0.4 for secondary iodides, and <0.05 for tertiary iodides. Specifically, for *n*-propyl iodide, the C−I fission branching fraction is 0.74 ± 0.05 and has no temperature dependence, while the value for isopropyl iodide is in the range of 0.3−0.4, with a slight temperature dependence. Their results were consistent with the semi ion-pair model for the molecular elimination transition state.[30]

Despite the large amount of work on the pyrolysis of alkyl iodides, direct experimental observation of both the molecular elimination and bond fission pathways has not been reported. The experimental approach of flash pyrolysis coupled to supersonic expansion and vacuum ultraviolet (VUV) photoionization mass spectrometry provides short reaction times to examine the initial steps of pyrolysis, supersonic cooling to minimize recombination and reactions of products and intermediates, and minimized ion fragmentation due to the low ionization photon energy.[31−34] More importantly, the bond fission and molecular elimination pathways in the initial stage of pyrolysis can be directly observed *simultaneously* in this work, with minimum complication from subsequent reactions.

Experimental Section

The thermal decomposition experiments were performed with an apparatus that has been previously described.[33] It makes use of a Wiley-MacLaren type linear time-of-flight mass spectrometer to observe pyrolysis products by means of photoionization. Ethyl iodide (99+%) was obtained from Aldrich, *n*-propyl iodide (99+%) and isopropyl iodide (98+%) were from Acros Organics. Perdueterated ethyl iodide (99+%) was obtained from Jansen Chimica and the mixed isotopomers of ethyl iodide (98+%) and propyl iodide (99+%) from CDN Isotopes. The compounds studied were used without further purification and diluted to 1−4% in argon or helium by bubbling the noble carrier gas through the liquid at ethylene glycol/dry ice or ice/water bath temperatures. The backing pressure of the gas mixture was maintained at ~1.5 atm for all experiments. The pyrolysis microreactor was based on the apparatus described by Chen and co-workers.[34] The thermal decompositions were carried out by expanding the gas mixture through a heated SiC nozzle (carborundum, heated length 10 mm, 2 mm o.d., 1 mm i.d.) which is attached to a machinable alumina piece that isolates the nozzle thermally and electrically from the pulsed valve. The nozzle was heated resistively by means of two press-fitted graphite electrodes with the current controlled by a Variac transformer. The temperature of the nozzle was measured with a type C (Omega) thermocouple wrapped around the exterior of the reaction zone previously calibrated to internal temperature. The gas flow properties in the SiC tube were investigated at elevated temperatures and at 1−2 atm backing pressure (i.e., under conditions similar to our experiment).[34,35] The speed of the sample flow is believed to be approximately sonic in the short heated region with a residence time of around 20−100 μs depending on the carrier gas utilized (e.g., ~20 μs for He and ~ 60 μs for Ar).[34,35] The gas pressure at the exit of the tube was still sufficient to produce a supersonic expansion and cooling; upon exit from the heated reaction zone the nascent products, intermediates, and any remaining reactants undergo supersonic expansion, which significantly reduces their internal energy content.[36] A molecular beam extracted from this expansion was then intercepted by 118.2 nm photons (10.49 eV) produced by frequency tripling of the 355 nm third harmonic of a Nd:YAG laser in a Xe cell (~20 Torr). The 118.2 nm light was focused by a MgF_2 lens through a small aperture into the photoionization region with concomitant divergence of the fundamental 355 nm source which minimized multiphoton ionization. The TOF spectra were collected using a multichannel plate detector and a digital oscilloscope (Tektronix) being averaged over 512 laser shots and then converted to mass spectra.

Results

1. Ethyl Iodide (CH_3CH_2I, CH_3CD_2I, CD_3CH_2I, and CD_3CD_2I). Stack plots of mass spectra for the low temperature pyrolysis of CH_3CH_2I, (2%) in argon carrier gas and (12%) in helium, are presented in Figure 1, parts a and b, respectively. Mass spectra for the high temperature pyrolysis of CH_3CH_2I in argon and helium (at the same concentrations) are presented in Figure 2, parts a and b. The mass spectra for the pyrolysis of isotopomers, CH_3CD_2I (2%) in argon, CD_3CH_2I (4%) in helium, and CD_3CD_2I (2%) in argon, are shown in Figure 3, parts a−c, respectively.

In Figure 1a, the spectral traces have heater temperatures of 295, 645, 770, 790, 810, and 840 K. At room temperature a large peak at *m/e* 156 due to molecular ion of the parent C_2H_5I [ionization energy (IE) = 9.33 eV[37]] is observed, with a small photofragment peak at *m/e* 29. The reported appearance energy (AE) of the $CH_3CH_2^+$ photoionization fragment from C_2H_5I is 10.44 eV,[38] close to the VUV photon energy. At a temperature of 645 K an attenuation of signal is caused by a drop in number density upon heating. As the temperature is increased to 770, 790, 810, and 840 K, peaks at *m/e* 127 and 128 corresponding

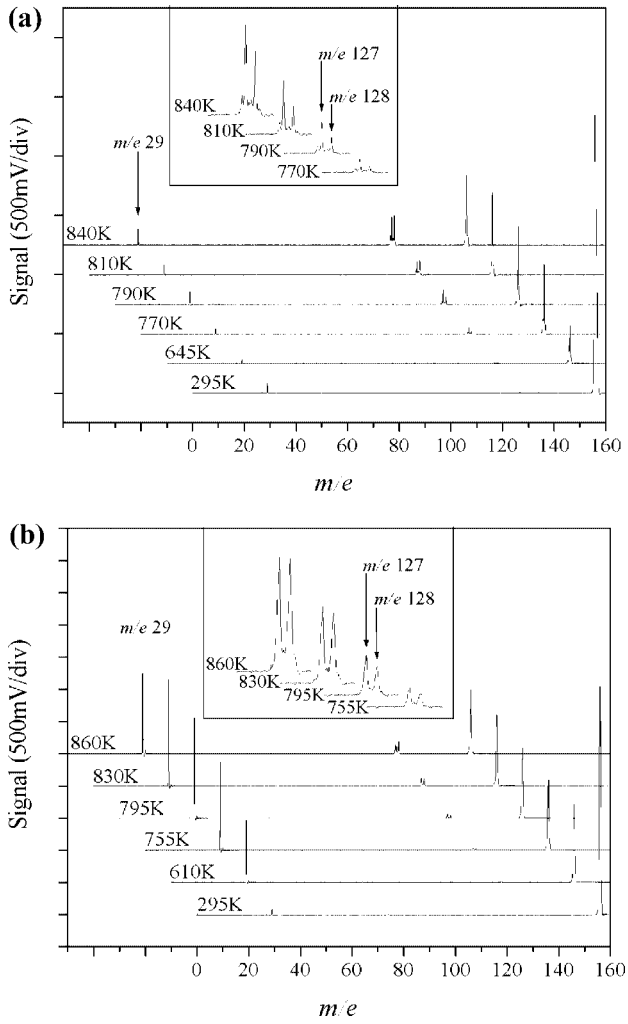

Figure 1. (a) Stack plot of mass spectra for pyrolysis of CH_3CH_2I (2%) in argon with internal nozzle temperatures from room temperature (295 K) to 840 K. (b) Stack plot of mass spectra for pyrolysis of CH_3CH_2I (12%) in helium with internal nozzle temperatures from room temperature (295 K) to 860 K. The mass spectra are shifted for clarity.

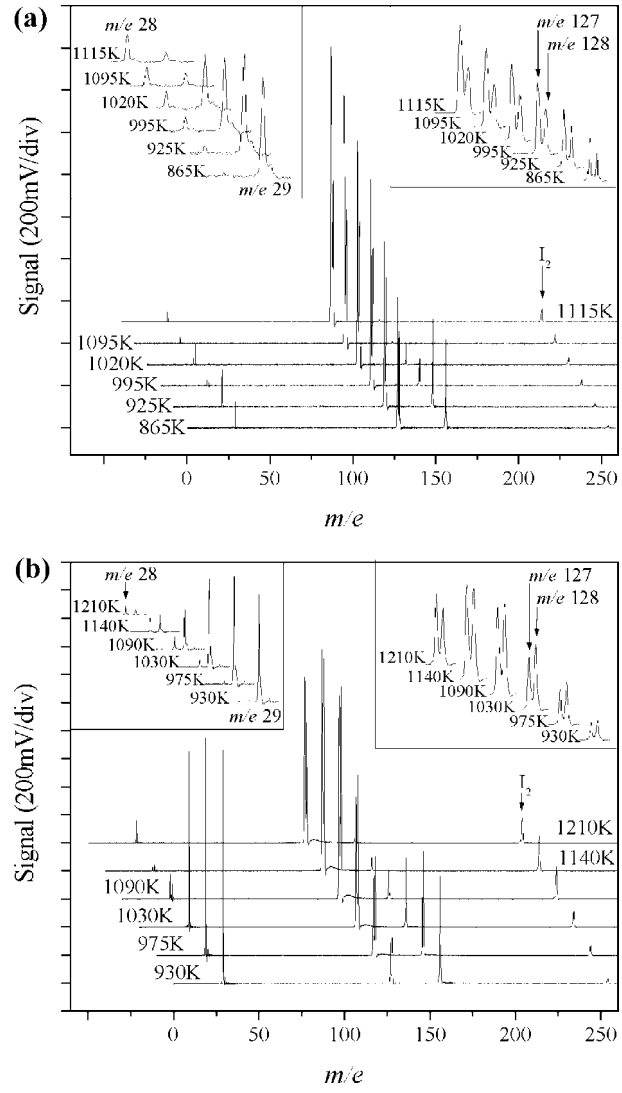

Figure 2. (a) Stack plot of mass spectra for pyrolysis of CH_3CH_2I (2%) in argon with internal nozzle temperatures from 865 to 1115 K. (b) Stack plot of mass spectra for prolysis of CH_3CH_2I (12%) in helium with internal nozzle temperatures from 930 to 1210 K. The mass spectra are shifted for clarity.

to iodine atom and hydrogen iodide are clearly discernible and drastically rise in intensity. Since the appearance energy of I^+ at *m/e* 127 from C_2H_5I is 14.8 eV,[39] this peak is therefore a result of photoionization of iodine atom (IE = 10.45 eV)[40] produced by homolytic cleavage of the C−I bond of C_2H_5I with a bond energy of ∼52.0 kcal/mol.[29,41] The AE for HI^+ is 11.7 eV,[39] too large to be observed as a photofragment in this system, and therefore the peak at *m/e* 128 is also due to photoionization of neutral HI created by thermolysis of C_2H_5I. The peak at *m/e* 29 increases in intensity over this temperature region. Direct photoionization of the neutral ethyl radical product in the C−I fission is readily accomplished in this system (IE = 8.12 eV[42]); however, $C_2H_5^+$ fragment due to photoionization fragmentation of C_2H_5I could also contribute to the *m/e* 29 signal. An additional consideration is that ethyl radicals rapidly decompose[29] into H atom (not detectable in this apparatus) and ethene which has an IE = 10.514 eV,[43] slightly higher than the ionization photon energy and not detectable in this modest temperature range. The mass spectra of CH_3CH_2I (12%) in helium at heater temperatures from 295 to 860 K are shown in Figure 1b. These mass spectra and their temperature dependence are similar to those in Ar shown in Figure 1a. However, at the elevated temperatures (>610 K), the relative intensity of the *m/e* 29 fragment peak (from photoionization fragment of the hot parent molecule and thermally produced ethyl radical) is larger compared to the *m/e* 156 molecular ion peak than in the argon spectra (Figure 1a). Also, the HI peak at *m/e* 128 is larger compared to the I atom peak at *m/e* 127 than in the argon spectra, with nearly the same intensity in the helium spectra above 830 K.

Figure 2a presents the pyrolysis of CH_3CH_2I (2%) in argon at higher heater temperatures from 865 to 115 K. At 865 K the molecular ion decreases in intensity while the *m/e* 29, 127, and 128 peaks all increase. As the temperature is raised to 925, 995, 1020, and then 1115 K, the parent peak continues to decrease, as does the *m/e* 29 signal. At these higher temperatures the parent compound rapidly decomposes, and at temperatures of 1020 K or greater, none survives. As the parent compound is pyrolyzed, the contribution of photoionization fragmentation at *m/e* 29 is reduced, but that due to thermolysis ethyl products should increase. However, as mentioned previously, ethyl radicals rapidly decompose and at higher temperatures little *m/e* 29 is detected. Over this high temperature range both *m/e* 127 and 128 peaks continue to increase, with *m/e* 127 being larger than the *m/e* 128 peak. Small peaks at *m/e* 28 and 254 appear, corresponding to ethene and molecular iodine, respectively.

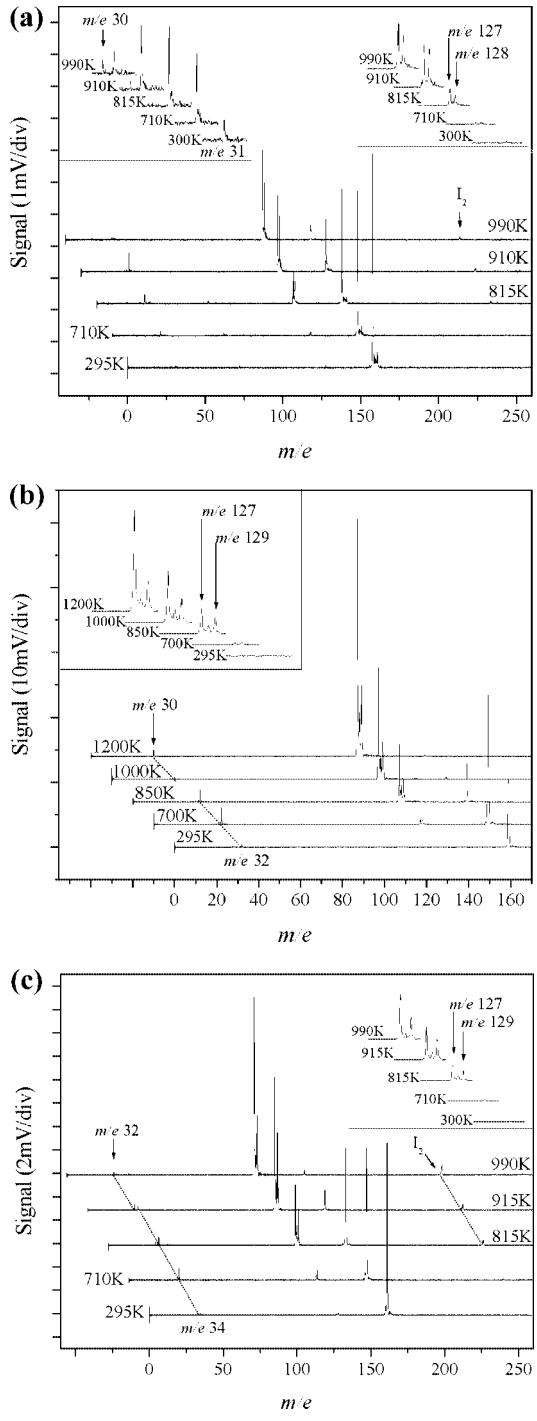

Figure 3. (a) Mass spectra for the pyrolysis of CH_3CD_2I (4%) in helium with heater temperatures of 300, 710, 815, 910, and 990 K. (b) Mass spectra for the pyrolysis of CD_3CH_2I (2%) in argon with heater temperatures of 295, 700, 850, 1000, and 1200 K. (c) Mass spectra for the pyrolysis of CD_3CD_2I with heater temperatures from 295 to 990 K.

Although the IE for ethene is slightly higher than the photoionization energy, at these high temperatures cooling becomes less complete and enough internal energy content may remain for a "warm" molecule of ethene to be detected. Figure 2b is for CH_3CH_2I (12%) in helium at higher temperatures from 930 to 1210 K. The trends are similar to those in the argon spectra in Figure 2a. As before, the *m/e* 29 peak has higher relative intensity compared to the molecular ion peak than in the argon spectra (Figure 2a), and this peak decreases with increasing temperature. Both the *m/e* 127 and 128 peaks drastically increase in intensity, with the HI peak being slightly higher compared to the I atom peak than in the argon spectra. The I_2 peak at *m/e* 254 starts around 930 K and increases with higher temperature. The small peak at *m/e* 28, C_2H_4, is observed and increases in intensity with the decreasing *m/e* 29 peak at higher temperatures. At the highest temperatures, *m/e* 127 and 128 are the dominant peaks.

Figure 3a shows the pyrolysis of partially dueterated isotopomer CH_3CD_2I (4%) in helium at temperatures of 300, 710, 815, 910, and 990 K. At room temperature, a strong molecular ion is observed at *m/e* 158, accompanied by a minor $CH_3CD_2^+$ photofragment at *m/e* 31. As 710K, the *m/e* 31 peak increases relative to the parent *m/e* 158 peak, indicating production of CH_3CD_2 from thermolysis of CH_3CD_2I. From 815 to 990 K, the I and HI peaks at *m/e* 127 and 128 grow significantly, while the molecular ion peak is drastically diminished. The *m/e* 31 peak decreases with the increasing temperatures, while a new *m/e* 30 peak appears above 910 K, indicating decomposition of the CH_3CD_2 radical to CH_2D_2. Also, a very small I_2 peak is observed at *m/e* 254 at the highest temperatures.

The pyrolysis of CD_3CH_2I (2%) in argon at temperatures 295, 700, 850, 1000 and 1200 K is presented in Figure 3b. The molecular ion is observed at *m/e* 159 at room temperature. At 700 K a CD_3CH_2 peak at *m/e* 32 is observed with approximately one-third the intensity of the molecular ion. Above 850 K the parent peak at *m/e* 159 is significantly reduced and becomes not detectable above 1000K. From 850 to 1200 K, the *m/e* 127 (I) and 129 (DI) peaks grow significantly and become dominant, with *m/e* 129 being approximately two-thirds to one-third of *m/e* 127; a small peak at *m/e* 128 is also observed along with these two peaks. Above 850 K, the *m/e* 32 peak decreases rapidly, while a small peak at *m/e* 30 is detected, indicating again that the CD_3CH_2 radical undergoes thermal decomposition to CD_2CH_2 + D.

Figure 3c shows the mass spectra of CD_3CD_2I (2%) in argon at nozzle temperatures of 300, 710, 815, 915, and 990 K. At room temperature a large molecular ion peak at *m/e* 161 is the only discernible peak. At 710 K the molecular ion is slightly diminished, and an *m/e* 34 peak is observed, along with small peaks at *m/e* 127 (I) and 128 (HI). Since no hydrogen is present in the fully dueterated sample (as the parent mass spectrum at room temperature indicates no impurity), the HI peak at *m/e* 128 should come from surface exchange reactions of DI with the silicon carbide microreactor. The *m/e* 34 peak is largely due to the CD_3CD_2 radical from the pyrolysis of CD_3CD_2I. At 815 K the *m/e* 34 peak continues growth, and the *m/e* 127 (I) and 129 (DI) peaks drastically increase, with the *m/e* 127 peak being approximately half-of *m/e* 129. The small peak at *m/e* 128 (HI) is still present. A peak at *m/e* 254 emerges corresponding to the molecular I_2. From 915−990 K, the peaks at *m/e* 34 and 161 quickly reduce in intensity and become barely detectable. A new peak arises at *m/e* 32, indicating the decomposition of CD_3CD_2 to CD_2CD_2, and the *m/e* 127 and 129 peak continue to increase while maintaining the same relative intensities. The peak at *m/e* 128 is still present, although, the relative intensity indicates the contribution of surface exchanged hydrogen iodide is minimal.

2. *n*-Propyl Iodide ($CH_3CH_2CH_2I$ and $CD_3CD_2CH_2I$). Mass spectra for pyrolysis of *n*-propyl iodide (1%) in argon at temperatures 295, 760, 845, 975, and 1065 K are presented in Figure 4a. The spectrum at 295 K has a molecular ion peak at *m/e* 170 (IE = 9.26 eV)[44] and a photoionization fragment $CH_3CH_2CH_2^+$ at *m/e* 43 (AE = 9.8 eV).[44] From 760 to 845 K, the parent peak decreases slightly with concomitant growth of the *m/e* 43 peak; a new peak at *m/e* 127 (I) appears, while a

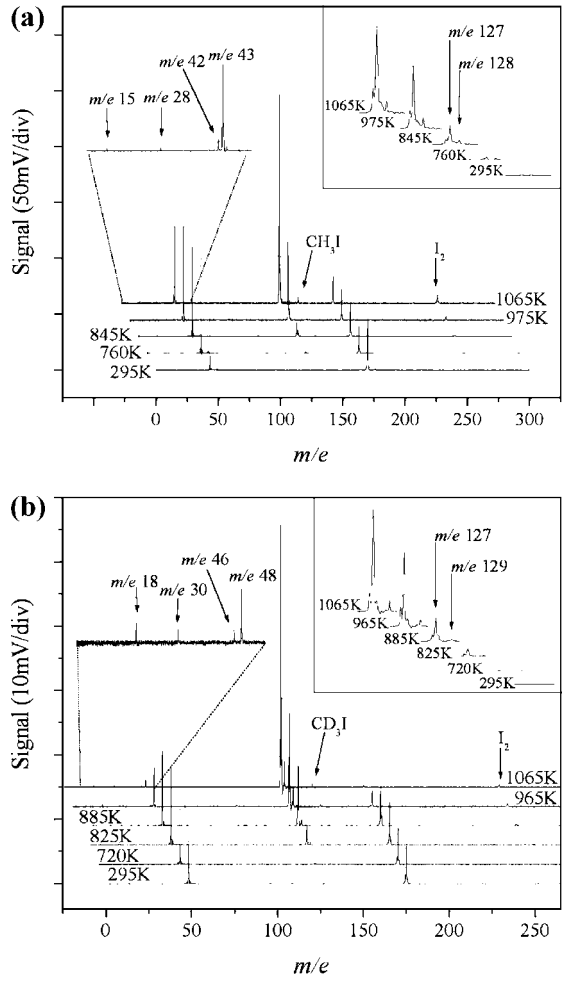

Figure 4. (a) Mass spectra for the pyrolysis of *n*-propyl iodide (1% in Ar) with heater temperatures from 295 to 1065 K. (b) Mass spectra for pyrolysis of the isotopomer $CD_3CD_2CH_2I$.

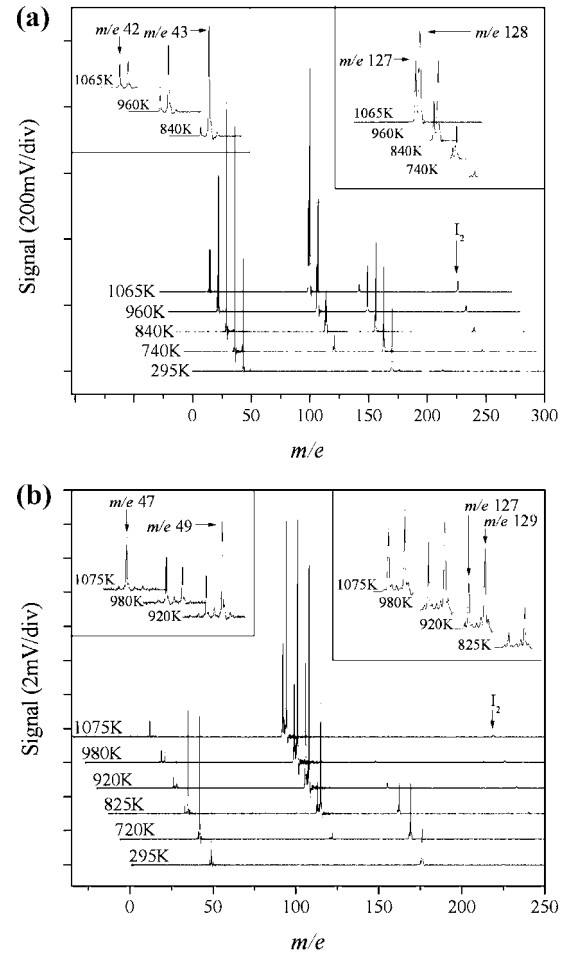

Figure 5. (a) Mass spectra for the pyrolysis of isopropyl iodide with heater temperatures from 295 to 1065 K. (b) Mass spectra for the pyrolysis of isotopomer CD_3CHICD_3 with heater temperatures from 295 to 1075 K.

small peak at *m/e* 128 (HI) is hardly detectable. From 975 to 1065 K, the *m/e* 170 and 43 peak attenuate slightly, while the *m/e* 127 and 128 peak grow dramatically. As HI^+ is not a reported photoionization fragment of *n*-propyl iodide, the *m/e* 128 peak is the HI product of thermal decomposition. At 1065 K, new peaks at *m/e* 42, *m/e* 28, and *m/e* 15 are detected correlating to propene, ethene, and methyl radical. The appearance of these peaks is consistent with decomposition of the *n*-propyl radical to ethene + methyl radical, which is known to occur in the conditions of very low pressure pyrolysis (VLPP) of *n*-propyl iodide,[21] and propene + H atom. A *m/e* 254 peak is detected as molecular iodine and increases with temperature. At 1065 K, a new peak at *m/e* 142 is observed corresponding to methyl iodide, CH_3I. At higher temperatures (not depicted here), the relative amounts of *m/e* 127 and 128 remain nearly constant. The *m/e* 15 and *m/e* 42 peaks are still detected as well as a small peak at *m/e* 28, while the *m/e* 43 peak disappears, indicating the complete decomposition of the *n*-propyl radicals at the higher temperatures. The *m/e* 254 peak also attenuates as I_2 undergoes secondary pyrolysis.

Figure 4b displays the pyrolysis of the isotopomer $CD_3CD_2CH_2I$ (1%) in argon at temperatures of 295, 720, 825, 965, and 1065 K. At 295 K the molecular ion peak *m/e* 175 is $\sim$ 70% the intensity of the $CD_3CD_2CH_2^+$ photoionization fragment at *m/e* 48, similar to the undeuterated sample. At 825 K, the *m/e* 48 peak increases over the molecular ion at *m/e* 175; a peak at *m/e* 127 (I) appears. From 885 to 1065 K, the parent peak at *m/e* 175 is greatly reduced, while the *m/e* 127 peak grows many times, along with a small peak at *m/e* 129 (DI) to approximately 10% of the *m/e* 127 intensity. No peak at *m/e* 128 is observed which indicates a negligible contribution from the surface hydrogen exchange reaction of DI produced in the gas phase. In addition, the *m/e* 48 peak is greatly attenuated, while small peaks at *m/e* 18, 30, and 46 are detected and increase with the temperatures, which corresponds to the decomposition of $CD_3CD_2CH_2$ to CD_3, CD_2CH_2, and CD_3CDCH_2, respectively. The *m/e* 18, 30, and 129 peaks are more readily detected for the isotopomer than in the undeuterated pyrolysis. The small peak at *m/e* 254 is due to I_2, and the small peak at *m/e* 145 is CD_3I.

3. Isopropyl Iodide (CH_3CHICH_3 and CD_3CHICD_3). The mass spectra of the pyrolysis of isopropyl iodide (2%) in argon at temperatures of 295, 740, 840, 960, and 1065 K are presented in Figure 5a. At 295 K, the parent peak *m/e* 170 (IE = 9.18 eV)[44] has approximately half the intensity of the photoionization fragment peak at *m/e* 43, $CH_3CHCH_3^+$ (AE = 9.70 eV).[44] At 740 K the *m/e* = 43 peak increases relative to the parent peak, and a new peak at *m/e* 128 (HI) appears. At 840 K the *m/e* 170 and *m/e* 43 peaks remain essentially unchanged while the *m/e* 128 peak increases over an order of magnitude. A small peak at *m/e* 127 (I), about 10% the intensity of the HI peak at *m/e* 128, is seen, and peaks at *m/e* 42 and 254 are visible correlating to product propene (IE = 9.73)[45] and I_2, respectively. From 960 to 1065 K, the *m/e* 170 parent peak reduces significantly in

intensity, while both the *m/e* 128 and 127 peaks increase greatly, with the *m/e* 127 peak being 50% to 75% of the *m/e* 128 peak. The *m/e* 254 peak continues to increase. The *m/e* 43 peak is also reduced in intensity as the *m/e* 42 peak grows, becoming equal in intensity to *m/e* 43 at 1065 K; this indicates decomposition of the isopropyl radical to propene. As found in the pyrolysis of *n*-propyl iodide, at even higher temperatures the parent peak at *m/e* 170 and the *m/e* 43 peak are no longer detectable, and the peaks at *m/e* 128 and 254 steadily decrease.

The pyrolysis mass spectra for CD_3CHICD_3 (2%) in argon at temperatures of 295, 720, 825, 920, 980, and 1075 K are shown in Figure 5b. At 295 K, the molecular ion at *m/e* 176 is about half the size of the photofragment, $CD_3CHCD_3^+$, at *m/e* 49, similar to the unlabeled compound. At 720 K the *m/e* 49 peak increases relative to the *m/e* 176 peak, and small new peaks at *m/e* 127 (I) and 129 (DI) are observed with *m/e* 129 being approximately double the intensity of *m/e* 127. At 825 K the molecular ion signal decreases significantly, the *m/e* 49 peak is of similar relative size in comparison to *m/e* 176, and new peaks at *m/e* 47 (isotopomer of propene, CD_3CHCD_2) and 254 (I_2) appear. The *m/e* 129 peak, DI, is now the largest one, growing by more than 1 order of magnitude, with a *m/e* 127 peak approximately a third of the *m/e* 129 peak. As the temperatures of 920, 980, and 1075 K the molecular ion at *m/e* 176 and the peak at *m/e* 49 disappear as the peaks at *m/e* 47, 127, and 129 increase in intensity. Over this temperature range a small I_2 peak at *m/e* 254 is detected.

Discussion

Comparison of parts a and b of Figure 1 illustrates the effects of carrier gases in this experimental technique that has been described previously.[32] The carrier gas affects the photoionization mass spectra in two ways: (1) the efficiency of sample cooling and (2) the residence time in the microreactor. Photoionization fragmentation is sensitive to the internal energy content of the parent molecules, especially when the AEs of the fragments are close to the photon energy, and here ethyl iodide is such an example ($C_2H_5^+$ AE = 10.44 eV[38] vs 10.49 eV photon energy). Although helium will cool a room temperature sample to <50 K rotational temperature,[36] after pyrolysis the cooling is less efficient from the high temperature. The heavier argon gas provides for more efficient cooling which thereby results in the suppression of photoionization fragmentation. This effect is evident when comparing the relative signals at *m/e* 29 in Figure 1, parts a and b, which are due to both photoionization fragmentation of C_2H_5I and photoionization of neutral C_2H_5 from C_2H_5I thermolysis. For both the argon and helium entrained samples a photoionization fragment at *m/e* 29 is hardly detectable when the samples are expanded and cooled from the room temperature nozzle. As heat is applied the extent of photoionization fragmentation remains minimal in the argon sample, and the growth of the *m/e* 29 peak is modest and seems to be mainly due to the C_2H_5I thermolysis. In contrast, in helium (with also higher C_2H_5I concentration) the photofragment peak at *m/e* 29 has significant increases, being almost equal in intensity to the parent mass peak M^+ at a nozzle temperature of only 610 K. In both samples growth of the *m/e* 29 peak is observed concomitant with the growth of *m/e* 127 and 128 as the nozzle is heated up to ~860 K. It may be that the amount of photoionization fragmentation over the 600−860 K temperature range is fairly consistent. If this is the case, the signal for thermally produced ethyl radicals that accompany the detected iodine atoms can be approximated by subtracting the intensity of the *m/e* 29 peak at the heater temperature of ~600−650 K from the *m/e* 29 signal at higher temperatures. One must also consider that the ethyl radical readily decomposes (ΔH = 34.8 kcal mol^{-1})[29] to H atom (not detectable in this study) and ethene (not detected at lower temperatures).

The effectiveness of cooling is also evident by comparing the peak intensities at *m/e* 127 and 128 in Figure 1, parts a and b. Note that the intensity of *m/e* 128 relative to 127 is smaller in the argon entrained sample in comparison to that in helium. I atom and HI have similar ionization energies (IE = 10.43 eV[46] for I and 10.38 eV[47] for HI); however, the sensitivities for their photoionization detection at higher temperatures in these pyrolysis experiments could be different due to the different dependence on the internal energies. I atoms lack rotational and vibrational energy to be cooled by supersonic expansion and are essentially always in the ground-state in both the argon and helium beams, while the ionization efficiency of HI is found to be sensitive to the extent of cooling of the internal energy. Helium provides less cooling for HI which results in a slightly more ionization in comparison with I atom whose ionization is not affected by cooling. In contrast, argon provides a greater degree of cooling for HI which results in a smaller peak with respect to I atom than in helium. The other factor affecting the sensitivity of I and HI detection is the residence time in the microreactor. The result of increased residence time is evident when comparing parts a and b of Figure 1. Note that the intensity of *m/e* 127 is less than 10% the parent M^+ peak at *m/e* 156 at 860 K in the helium, while in the argon data at 840 K the *m/e* 127 peak is greater than half-the M^+ intensity. The greater cooling ability of argon and the sensitivity for detection of HI at *m/e* 128 has been discussed above. From this one would expect less intense signals at *m/e* 127 and 128 in argon. The velocity through the microreactor is approximately sonic and therefore argon has a longer residence time, roughly three times that of helium. As a result, it is plausible that the difference is due to longer reaction time and more heat transferred to the pyrolysis sample in the flow of a heavier Ar carrier gas (with the same heat capacity or less). The very small I_2 peak (from secondary reactions) in argon (Figure 2a), due to the short residence time (~60 μs) and the low CH_3CH_2I concentration (2% in argon vs 12% in helium), indicates that the secondary reactions are minimum (despite 3 times longer residence time than in helium); and therefore the secondary reactions should not contribute significantly to the large *m/e* 127 and 128 peaks (with respect to the parent M^+ peak) in the argon spectrum (Figure 1a). In summary, the mass spectra in argon carrier gas are less sensitive to the internal energy and are thus used for subsequent analysis and discussion.

The pyrolysis of ethyl iodide was long believed to proceed primarily via molecular elimination due to the inconsistency of first order kinetics with the rate laws observed for other primary alkyl iodides. However, the more recent studies indicated that in the temperature range of 950−1400 K bond fission is the dominant process,[29,30] which is consistent with the semi-ion pair transition state theory.[22,23] And based on the recently reported kinetic parameters,[29,30] the C−I fission branching fraction increases slightly with temperature over 950−1400 K. Our data clearly show both the HI and I production, and thus the HI + ethene and I + ethyl radical channels (Figures 1 and 2). In the temperature range of 770−1100 K in this study, the C−I fission is observed to be slightly more than the molecular elimination. The C−I fission branching fraction (from the argon data) is plotted as a function of temperature in Figure 6a. The average C−I fission branching fraction is 0.7 ± 0.1 (1σ) in the temperature range of 770−1200 K, with a modest temperature

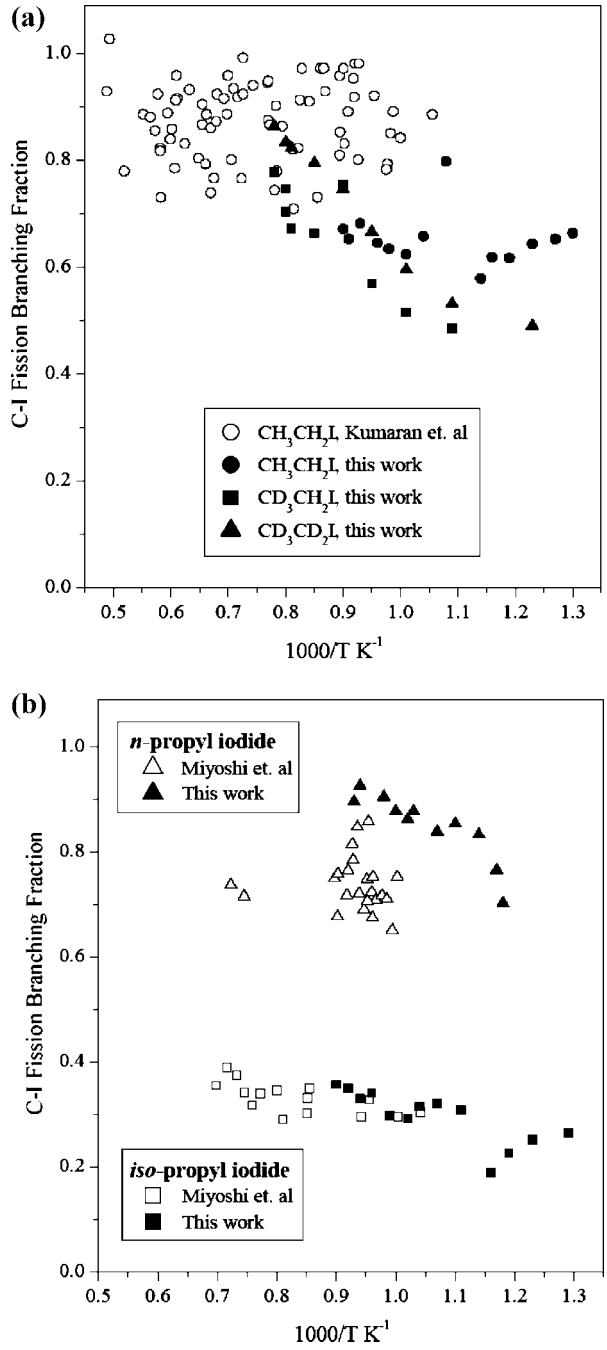

Figure 6. C−I bond fission branching fractions (not rescaled with the photoionization cross sections, see text for more details). (a) Branching fraction for ethyl iodide: Kumaran et. al (○, ref 29), CH_3CH_2I in this work (●),CD_3CH_2I in this work (■), and CD_3CD_2I in this work (▲). (b) Branching fraction for *n*-propyl iodide: Miyoshi et. al (Δ, ref 30) and this work (▲); branching fraction for isopropyl iodide: Miyoshi et al. (□, ref 30) and this work (■)].

dependence. This fraction is based on an assumption that the ionization cross sections of I and HI are comparable. Indeed, the photoionization cross section of HI at 118.2 nm, σ_{HI}, is ∼45 × 10^{-18} cm^2 (an average value from three references),[48−50] and that of the I atom at 118.2 nm, σ_I, is estimated to be in the range of 50−100 × 10^{-18} cm^2 by scaling experimental relative cross sections with theoretical calculations,[51−54] with the lower value of 50 × 10^{-18} cm^2 being more likely.[51−53] The average C−I fission branching fraction can then be rescaled to be 0.68 ± 0.1 with $\sigma_I \sim 50 \times 10^{-18}$ cm^2 or 0.51 ± 0.1 with $\sigma_I \sim 100 \times 10^{-18}$ cm^2. The issue of the photoionization cross sections will be discussed further with the propyl iodide results. The fraction is also an upper limit as there is a minor loss of I atoms due to the I_2 production or some undetected reactions of I atoms (although these are minimized by the short contact time). Our branching fraction is reasonably close to that by Kumaran et al. in Figure 6a[29] and the value of 0.92 ± 0.06 in the temperature range of 950−1400 K by Miyoshi et al.,[30] with our values being smaller than these two previous studies and having a modest temperature dependence. The *m/e* 29 peak increases initially to the maximum around 900−1000 K, and then decays at the higher temperatures, while the parent mass peak M^+ steadily decreases for the entire range. It is difficult to access the relative contributions to the *m/e* 29 peak from photoionization fragmentation and thermolysis of C_2H_5I (the coproduct of I atom); furthermore, at the higher temperature the ethyl radicals readily decompose to H + ethene. Nevertheless, the steady increase of the *m/e* 29 peak up to ∼1000 K, concomitant with the decrease of the parent mass peak, especially in the argon spectra where the C_2H_5I concentration is lower and supersonic cooling is more efficient, implies a major contribution from the neural thermolysis and supports the direct observation of ethyl radical from thermolysis. The coproduct of HI in the molecular elimination channel is ethene. At the temperatures below 840 K, no ethene *m/e* 28 peak is observed, possibly due to the slightly higher IE of ethene (10.514 eV)[43] than the photon energy and cooling of the ethene product. At temperatures >865 K, *m/e* 28 peak is detected, accompanying decreasing ethyl peak. This ethene product is more likely from decomposition of ethyl radical product rather than the coproduct of HI molecular elimination. This is because that in the high temperature region the ethene peak increases with temperature much faster than the HI peak, while the ethyl radical is known to readily decompose to H + ethene and indeed its peak decreases with the increasing temperature and ethene peak concomitantly. For ethene to be detected in this system, a small amount of internal energy (≥0.02 eV) need remain after the supersonic expansion. It is plausible that the ethene produced from ethyl is hotter and the cooling at the high temperatures is less complete. A small amount of I_2 is observed at high temperatures; the possible sources are recombination of I atoms and/or abstraction reaction of I + C_2H_5I.

Molecular elimination in the pyrolysis of alkyl iodides is thought to proceed via a C1, C2 mechanism (1,2 intramolecular elimination) instead of 1,1 as the transition state energy barrier for 1,1 molecular elimination has been shown to be prohibitive theoretically for the alkyl chlorides and bromides.[4] The exclusive observation of HI in the pyrolysis of CH_3CD_2I (Figure 3a) clearly illustrates that 1,1 molecular elimination is not occurring in the pyrolysis of ethyl iodide. The pyrolysis data of CD_3CH_2I and CD_3CD_2I in Figure 3, parts b and c support this conclusion and also illustrate a small contribution of DI exchange with the surface of the microreactor. The perdeuterated ethyl iodide contains no hydrogen and therefore any HI detected here must be the result of DI exchange reaction with hydrogen residing on the microreactor surface (which is known to occur readily). Since it is established from the early work[4] and our CH_3CD_2I results that the 1,1 molecular elimination is not feasible in ethyl iodide, the HI detected in the CD_3CH_2I experiment must come from another source such as the surface reactions (although a minor process); as the CD_3CD_2I data show that DI can produce HI via the surface exchange, the small HI signal in the CD_3CH_2I experiment can be readily explained by the surface exchange of DI (produced from 1,2 molecular elimination of CD_3CH_2I). These studies of the isotopomers also confirm the mechanisms of the ethyl iodide pyrolysis, which undergoes competitive bond

fission and unimolecular decomposition, with the C−I fission being more abundant and ethyl radicals (CH_3CH_2, CH_3CD_2, CD_3CH_2, and CD_3CD_2) produced decomposing further to H/D + ethene at higher temperatures.

In the pyrolysis of *n*-propyl iodide, $CH_3CH_2CH_2I$ has been known to primarily undergo bond fission and under low pressure conditions the resulting propyl radicals rapidly decompose into propene + H and ethene + CH_3.[21,30] The pyrolysis mass spectra of $CH_3CH_2CH_2I$ (Figure 4a) show that the thermal decomposition onsets around 750 K, and proceeds essentially exclusively through bond fission (*n*-propyl + I), with a minor amount of HI (molecular elimination HI + propene). The C−I fission branching fraction of *n*-propyl iodide is shown in Figure 6b. The average value is 0.85 ± 0.06 (1σ) in the temperature range of 850−1100 K, with the fraction increasing slightly over the temperatures. The average branching fraction can be rescaled to be 0.83 with $\sigma_I \sim 50 \times 10^{-18}$ cm^2 or 0.72 with $\sigma_I \sim 100 \times 10^{-18}$ cm^2. Our results are compared with those by Miyoshi et al. in Figure 6b (with an average of 0.74 ± 0.05),[30] and they are in reasonable agreement. The pyrolysis mass spectra of $CD_3CD_2CH_2I$ (Figure 4b) are similar, with a predominant I atom peak, a minor DI peak, and no HI signal; this clearly indicates that the molecular elimination is mainly via the C1, C2 elimination pathway in *n*-propyl iodide. A significant amount of photoionization fragmentation into *m/e* 43 $C_3H_7^+$ is due to the lower AE; nevertheless, the *m/e* 43 increases with the temperature, consistent with the *n*-propyl + I bond fission channel. Although difficult to detect, above ∼1000K the *n*-propyl radical is observed to decompose into methyl radical at *m/e* 15 and ethene at *m/e* 28, as well as to propene at *m/e* 42 + H (not detected). This decomposition process is more clearly observed in the pyrolysis of isotopomer $CD_3CD_2CH_2I$ (Figure 4b). A minor I_2 peak is observed similar to ethyl iodide. Interestingly, a small peak of CH_3I in the pyrolysis of $CH_3CH_2CH_2I$ and CD_3I in $CD_3CD_2CH_2I$ are identified, while these products are not detected in the pyrolysis of CH_3CHICH_3 and CD_3CHICD_3 (Figure 5). Several sources of the methyl iodide product are plausible: recombination reaction of CH_3 and I, CH_3 abstraction reaction with *n*-propyl iodide, or a (postulated) four-center elimination process in *n*-propyl iodide. These mechanisms are consistent with the fact that methyl iodide product are not detected in isopropyl iodide, as CH_3 is not a secondary product of isopropyl and isopropyl iodide does not have the four-center elimination to produce methyl iodide. The four-center elimination process in *n*-propyl iodide might be possible, as the methyl iodide product appears at lower temperature before the secondary CH_3 product.

In contrast to the *n*-propyl system, the pyrolysis of isopropyl iodide CH_3CHICH_3 is expected to primarily decompose into HI and propene via 1,2-ϵ_i.[30] The pyrolysis mass spectra of CH_3CHICH_3 in Figure 5a indicate that the thermal decomposition onsets around 700 K, and molecular elimination is preferred over bond fission over the temperature range studied. The C−I fission branching fraction of isopropyl iodide is shown in Figure 6b. The average value is 0.30 ± 0.05 (1σ) in the temperature range of 770−1100 K, with the fraction increasing slightly over the temperatures. The average branching fraction can be rescaled to be 0.28 with $\sigma_I \sim 50 \times 10^{-18}$ cm^2 or 0.16 with $\sigma_I \sim 100 \times 10^{-18}$ cm^2. Our results (without rescaling or rescaled with $\sigma_I \sim 50 \times 10^{-18}$ cm^2) are in good agreement with those by Miyoshi et al.[30] in Figure 6b, and this implies that the ionization cross sections of HI and I at 10.49 eV are nearly the same. The pyrolysis mass spectra of CD_3CHICD_3 (Figure 5b) are also similar, with competing I and DI product signals but no HI peak, further supporting that the molecular elimination in alkyl iodides is predominantly via the C1, C2 elimination pathway. A significant amount of photoionization fragmentation into *m/e* 43 $C_3H_7^+$ is also seen due to the lower AE. The *m/e* 43 peak increases with the temperature up to ∼800 K, consistent with the isopropyl + I dissociation. The isopropyl *m/e* 43 peak then falls significantly at temperatures >850 K, and concomitantly the propene product at *m/e* 42 is detected above ∼800 K and increases with temperatures. The production of propene are due to direct 1,2-ϵ_i of HI and/or secondary thermal decomposition of the isopropyl radicals. The observation of CD_3CHCD_3 and CD_3CHCD_2 in the CD_3CHICD_3 sample also supports this mechanism.

Our C−I fission branching fractions of ethyl iodide and propyl iodides are largely based on the I^+ and HI^+ peaks assuming the same ionization cross sections for I and HI. The agreement of our isopropyl iodide results with those by Miyoshi et. al (Figure 6b) would indicate that the ionization cross sections of I and HI are the same at 10.49 eV, while the comparison of ethyl iodide in Figure 6a would imply that the 10.49 eV photoionization cross section of HI would have to be ∼×4 of that of I in order for our fraction value to be ∼0.9. Moreover, the estimated 118.2-nm photoionization cross sections of HI and I, although with large uncertainty, indicate that the 10.49 eV photoionization cross section of HI is in the range of 0.5−1 of that of I.[48−54] Since both the *n*- and isopropyl iodide results are in better agreements with the previous studies by Miyoshi et. al,[30] and these are more consistent with the estimated photoionization cross sections from the literature, it is likely that the difference between our ethyl iodide results and those by Kumaran et. al[29] and Miyoshi et. al[30] are not due to the ionization cross sections of I and HI. In the context of the semi-ion pair transition state theory it is interesting that for the data presented in this work ethyl iodide undergoes 1,2-ϵ_i to a large extent at the elevated temperatures, while the C−I bond fission is always dominant in *n*-propyl iodide. The C−I bond dissociation energies for ethyl, *n*-propyl and isopropyl iodides are all nearly isoenergetic, being within ∼0.5 kcal/mol of each other;[30] furthermore, ethyl, *n*-propyl and isopropyl iodides have nearly the same pre-exponential A factors for the C−I bond fission. Consequently, the difference of the C−I fission branching fraction is determined by the relative rates of the 1,2−ϵ_i channel in the three compounds. Although *n*-propyl iodide has a σ value (symmetry number) that is $^2/_3$ of ethyl iodide, the presence of a β-methyl group should accentuate the rate of 1,2−ϵ_i.[1] However, when one compares the ratio of pre-exponential A factors for 1,2−ϵ_i versus bond fission from the recent calculations[29,30] a ratio of ∼0.4 is found for both ethyl and isopropyl iodides while for *n*-propyl iodide that ratio is only ∼0.2. In ethyl iodide and *n*-propyl iodide, both primary alkyl iodides, the activation energies for the 1,2−ϵ_i process are lowered by ∼15 kJ/mol compared to their C−I bond dissociation energies. For the secondary isopropyl iodide the activation energy for 1,2−ϵ_i is calculated to be 30 kJ/mol lower than the C−I bond fission. As a result, the 1,2−ϵ_i process is competitive with the C−I bond fission in the elevated temperatures for ethyl iodide despite being a primary alkyl halide, while the primary *n*-propyl iodide decomposes predominantly by bond fission and secondary isopropyl iodide decomposes primarily by 1,2−ϵ_i.

Conclusion

Pyrolysis of ethyl iodide onsets at ∼750 K. The C−I bond fission and HI 1,2 molecular elimination pathways are competitive over the elevated temperature range from 750−1200 K,

SCHEME 1: Schematic Depicting Initiation Events in the Pyrolysis of Alkyl Halides

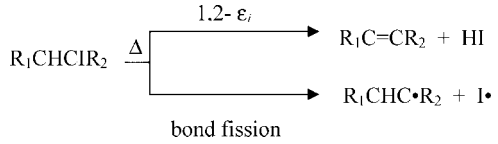

with the C−I bond fission being about ×2 of 1,2 molecular elimination pathway. The C−I fission branching fraction is in reasonable agreement with the previous studies and increases with the temperature. At temperatures above 1000 K, the ethyl radicals produced in the C−I fission undergo further decomposition into H + ethene, consistent with the previous reports. Molecular iodine is detected at temperatures >850 K. The photoionization fragmentation of ethyl iodide is sensitive to cooling of its internal energy, as shown in the comparison of mass spectra in helium and argon carrier gases.

The pyrolysis of *n*-propyl iodide onsets at ∼750 K, and the C−I bond fission dominates at the elevated temperature range of 700−1100 K. At temperatures greater than ∼950 K *n*-propyl radicals from the C−I fission decompose to ethene + methyl radical and propene + H. The I_2 product is detected above ∼850 K and the CH_3I product is detected above ∼900 K. In contrast, the isopropyl iodide pyrolysis onsets at ∼700 K; both HI and I products are observed, and the 1,2 molecular elimination pathway is preferred to bond fission at all temperatures presented. The isopropyl radicals from the C−I fission channel further decompose to propene + H at temperatures ≥850 K. The I_2 product is detected above ∼850 K but no CH_3I is detected. The C−I fission branching fraction of both *n*-propyl iodide and isopropyl iodide are in good agreement with the previous studies and increase slightly with the increasing temperature.

In all the three systems, isotopomer experiments verify that (1) the HI molecular elimination in ethyl and propyl iodides proceeds by a 1,2 molecular elimination mechanism as opposed to a 1,1 elimination, which has been demonstrated as prohibitive for alkyl chlorides and bromides theoretically, and (2) a minimal surface exchange of DI occurs on the surface of the microreactor.

Acknowledgment. This work was supported by the University of California Energy Institute and by NSF Grant CHE-0416244.

References and Notes

(1) Maccoll, A. *Chem. Rev.* **1969**, *69*, 33.
(2) Kim, K. C.; Setser, D. W. *J. Phys. Chem.* **1973**, *77*, 2021.
(3) Beiderhase, T.; Hoyermann, K.; Nothdurft, J.; Olzmann, M. *Z. Phys. Chem.* **2004**, *218*, 493.
(4) McGrath, M. P.; Rowland, F. S. *J. Phys. Chem. A* **2002**, *106*, 8191.
(5) Wolf, S.; Kim, C.-K. *Isr. J. Chem* **1993**, *33*, 295.
(6) Toto, J. L.; Pritchard, G. O.; Kirtman, B. *J. Phys. Chem.* **1994**, *98*, 8359.
(7) Glass, J. V. S.; Hinshelwood, C. N. *J. Chem. Soc.* **1929**, 1815.
(8) Jones, J. L.; Ogg, R. A. *J. Am. Chem. Soc.* **1937**, *59*, 1939.
(9) Jones, J. L.; Ogg, R. A. *J. Am. Chem. Soc.* **1937**, *59*, 1931.
(10) Butler, E. T.; Polanyi, M. *Trans. Faraday Soc.* **1943**, *39*, 19.
(11) Benson, S. W. *J. Chem. Phys.* **1963**, *38*, 1945.
(12) O'Neal, H. E.; Benson, S. W. *J. Chem. Phys.* **1961**, *34*, 514.
(13) Bose, A. N.; Benson, S. W. *J. Chem. Phys.* **1963**, *38*, 1945.
(14) Hartley, D. B.; Benson, S. W. *J. Chem. Phys.* **1963**, *39*, 132.
(15) Nangia, P. S.; Benson, S. W. *J. Chem. Phys.* **1964**, *41*, 530.
(16) Nangia, P. S.; Benson, S. W. *J. Am. Chem. Soc.* **1964**, *86*, 2773.
(17) Golden, D. M.; Rodgers, A. S.; Benson, S. W. *J. Am. Chem. Soc.* **1966**, *88*, 3196.
(18) Benson, S. W.; O'Neal, H. E., *Kinetic Data on Gas Phase Unimolecular Reactions,* National Standard Reference Data Service, U. S. National Bureau of Standards; Washington, DC, 1970.
(19) Teranishi, H.; Benson, S. W. *J. Chem. Phys.* **1964**, *40*, 2946.
(20) Bose, A. N.; Benson, S. W. *J. Chem. Phys.* **1962**, *37*, 2935.
(21) King, K. D.; Golden, D. M.; Spokes, G. N.; Benson, S. W. *Int. J. Chem. Kinet.* **1971**, *111*, 411.
(22) Benson, S. W.; Bose, A. N. *J. Chem. Phys.* **1963**, *39*, 3463.
(23) Benson, S. W.; Haugen, G. R. *J. Am. Chem. Soc.* **1965**, *87*, 4036.
(24) Tsang, W. *J. Chem. Phys.* **1964**, *41*, 2487.
(25) Yang, J. H.; Conway, D. C. *J. Chem. Phys.* **1965**, *43*, 1296.
(26) Choudhary, G.; Holmes, J. L. *J. Chem. Soc. B* **1968**, 1265.
(27) Herzler, J.; Frank, P. *Ber. Bunsenges. Phys. Chem.* **1992**, *96*, 1333.
(28) Mertens, J. D.; Wooldridge, M. S., Hanson, R. K. *Eastern States Section Technical Meeting*, The Combustion Institute: Pittsburgh, PA 1994.
(29) Kumaran, S. S.; Su, M.-C.; Lin, K. P.; Michael, J. V. *26th Symp. (Int.) Combust.* **1996**, *26*, 605.
(30) Miyoshi, A.; Yamauchi, N.; Kosaka, K.; Koshi, M.; Matsui, H. *J. Phys. Chem. A* **1999**, *103*, 46.
(31) Chambreau, S. D.; Lemieux, J.; Wang, L.; Zhang, J. S. *J. Phys. Chem. A* **2005**, *109*, 2190.
(32) Weber, K. H.; Zhang, J. S.; Borchardt, D.; Morton, T. H. *Int. J. Mass Spectrom.* **2006**, *249*−*250*, 303.
(33) Weber, K. H.; Zhang, J. S. *J. Phys. Chem. A* **2007**, *111*, 11487.
(34) Kohn, D. W.; Clauberg, H.; Chen, P. *Rev. Sci. Instrum.* **1992**, *63*, 4003.
(35) Friderichsen, A. V.; Radziszewski, J. G.; Nimios, M. R.; Winter, P. R.; Dayton, D. C.; David, D. E.; Ellison, G. B. *J. Am. Chem. Soc.* **2001**, *123*, 1977.
(36) Clauberg, H.; Minsek, D. W.; Chen, P. *J. Am. Chem. Soc.* **1992**, *114*, 99.
(37) Watanabe, K. *J. Chem. Phys.* **1964**, *41*, 1469.
(38) Traeger, J. C.; McLoughlin, R. G. *J. Am. Chem. Soc.* **1981**, *103*, 3647.
(39) Irsa, A. P. *J. Chem. Phys.* **1957**, *26*, 18.
(40) Lide, D. R. *Handbook Chem. Phys.* **1992**, 10–211.
(41) Sullivan, J. H. *J. Phys. Chem.* **1961**, *65*, 722.
(42) Ruscic, B.; Berkowitz, J.; Curtiss, L. A. *J. Chem. Phys.* **1989**, *91*, 114.
(43) Williams, B. A.; Cool, T. A. *J. Am. Chem. Soc.* **1991**, *94*, 6358.
(44) Traeger, J. C. *Int. J. Mass Spectrom Ion Phys.* **1980**, *32*, 309.
(45) Traeger, J. C. *Int. J. Mass Spectrom Ion Proc.* **1984**, *58*, 259.
(46) Grade, M.; Rosinger, W. *Sur. Sci.* **1985**, *156*, 920.
(47) Watanabe, K. *J. Chem. Phys.* **1957**, *26*, 542.
(48) Carlson, T. A.; Gerard, P.; Pullen, B. P.; Grimm, F. A. *J. Chem. Phys.* **1988**, *89*, 1464.
(49) Hart, D. J.; Hepburn, J. W. *Chem. Phys.* **1989**, *129*, 51.
(50) Boewering, N.; Mueller, M.; Salzmann, M.; Heinzmann, U. *J. Phys. B: At., Mol. Opt. Phys.* **1991**, *24*, 4793.
(51) Manson, S. T.; Msezane, A.; Starace, A. F.; Shahabi, S. *Phys. Rev. A* **1979**, *20*, 1005.
(52) Berkowitz, J.; Batson, C. H.; Goodman, G. L. *Phys. Rev. A* **1981**, *24*, 149.
(53) Robicheaux, F.; Greene, C. H. *Phys. Rev. A* **1992**, *46*, 3821.
(54) Taatjes, C. A.; Osborn, D. L.; Selby, T. M.; Meloni, G.; Fan, H.; Pratt, S. T. *J. Phys. Chem. A* **2008**, *112*, 9336.

JP808155A